Complexity Fusion for Indexing Reeb Digraphs

Francisco Escolano[1], Edwin R. Hancock[2], and Silvia Biasotti[3]

[1] University of Alicante
sco@dccia.ua.es
[2] University of York
erh@cs.york.ac.uk
[3] CNR-IMATI Genova
silvia@ge.imati.cnr.it

Abstract. In this paper we combine different quantifications of heat diffusion-thermodynamic depth on digraphs in order to match directed Reeb graphs for 3D shape recognition. Since different real valued functions can infer also different Reeb graphs for the same shape, we exploit a set of quasi-orthogonal representations for comparing sets of digraphs which encode the 3D shapes. In order to do so, we fuse complexities. Fused complexities come from computing the heat-flow thermodynamic depth approach for directed graphs, which has been recently proposed but not yet used for discrimination. In this regard, we do not rely on attributed graphs as usual for we want to explore the limits of pure topological information for structural pattern discrimination. Our experimental results show that: a) our approach is competitive with information-theoretic selection of spectral features and, b) it outperforms the discriminability of the von Neumann entropy embedded in a thermodynamic depth, and thus spectrally robust, approach.

1 Introduction

This paper is motivated by the hypothesis that mixing the same graph complexity measure over the same shape, represented with different graphs boosts the discrimination power of isolated complexity measures. To commence, there has been a recent effort in quantifying the intrinsic complexity of graphs in their original discrete space. Early attempts have incorporated principles related to MDL (Minimum Description Length) to trees and graphs (see [1] for trees and [2] for edge-weighted undirected graphs). More recently, the intersection between structural pattern recognition and complex networks has proved to be fruitful and has inspired several interesting measures of graph complexity. Many of them rely on elements of spectral graph theory. For instance, Passerini and Severini have applied the quantum (von Neumann) entropy to graphs [3]. We have recently applied thermodynamic depth [5] to the domain of graphs [6] and we have extended the approach to digraphs [7]. However, this latter approach has not been applied to graph discrimination as the one based on approximated von Neumann entropy [4]. Simultaneously, we have recently developed a method for selecting the best set of spectral features in order to classify Reeb graphs

R. Wilson et al. (Eds.): CAIP 2013, Part I, LNCS 8047, pp. 120–127, 2013.

(which summarize 3D shapes) [8]. Besides the spectral features we have evaluated in the latter work the discriminability of three different real functions for building Reeb graphs: geodesic, distance from barycenter and distance from the circumscribing sphere. Feature selection results in two intriguing conclusions: a) heat flow complexity is not one of the most interesting features, and b) the three latter real functions for building Reeb graphs have a similar relevance. The first conclusion seems to discard the use of heat flow based complexity measures for discrimination, at least in undirected graphs, whereas the second conclusion points towards discarding also the analysis of the impact of the representations. In this paper we show that these conclusions are misleading. To commence, when directed graphs are considered, heat-flow complexity information is richer. Secondly, the three functions explored in [8] are far from being orthogonal (they produce very similar graphs). Consequently herein we fuse both lines of research in order to find the best performance achievable only with topological information (without attributes). In Section 2 we present the catalog of real functions we are going to explore. In Section 3 we highlight the main ingredients of heat flow and thermodynamic depth in digraphs. Section 4 is devoted to analyze the result of fusing the directed complexities of several Reeb graphs from the same 3D shape. Finally, in Section 5 we will present our conclusions and future works.

2 Directed Reeb Graphs and Real Functions

The Reeb graph [9] is a well-known topological description that codes in a graph the evolution of the isocontours of a real-valued, continuous function $f : M \to \mathbf{R}$ over a manifold M. In other words, it tracks the origin, the disappearance, the union or the split of the isocontours as the co-domain of the function f is spanned. The nodes of the Reeb graph correspond to the critical points of f while the arcs are associated to the surface portions crossed when going from a critical points to another.

Several algorithms exist for the Reeb graph extraction from triangle meshes [10]; in this paper we adopt a directed version of the Extended Reeb graph (ERG) [11], we name it, the *diERG*. The diERG differs from the ERG in terms of arc orientation. Similarly to the ERG, to build the diERG we sample the co-domain of f with a finite number of intervals, then we characterize the surface in term of critical or regular areas and, finally, we track the evolution of the regions in the graph. Arcs are oriented according to the increasing value of the function. The diERG is then an acyclic, directed graph, a formal proof of this fact can be found in [12]. Figure 1 shows the pipeline of the graph extraction.

Each function can be seen as a geometric property and a tool for coding invariance in the description [13]. When dealing with shape retrieval, the function f has to be invariant from object rotation, translation and scaling. In the large number of functions available in the literature, we are considering:

- the distance from the barycentre B of the object, $Bar(p) = d_E(p, B)$, $p \in M$ and d_E represents the usual Euclidean distance (Figure 2-b);

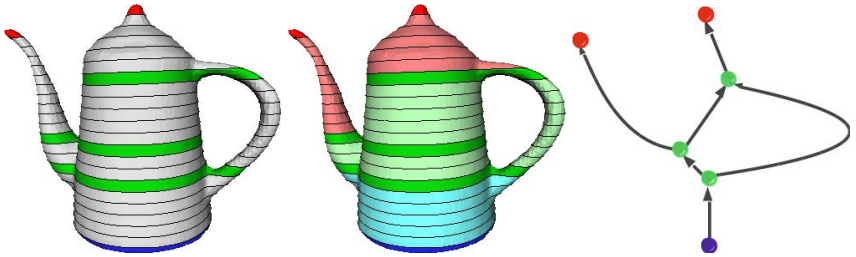

Fig. 1. Pipeline of the diERG extraction. (a) Surface partition and recognition of critical areas; blue areas correspond to minima, red areas correspond to maxima, green areas to saddle areas. (b) Expansion of critical areas to their nearest one. (c) The oriented diERG.

- the distance from the main shape axis $\boldsymbol{v}$, $MSA(p) = d_E(p, \boldsymbol{v})$, (Figure 2-c);
- the function $MSANorm(p) = \|\boldsymbol{v} \times (p - B)\|$, $p \in S$, $\boldsymbol{v}$ is the same as above and B is the barycentre (Figure 2-d);
- the average of the geodesic distances defined in [14] (Figure 2-e);
- the first six (ranked with respect to the decreasing eigenvalues), non-constant eigenfunctions of the Laplace-Beltrami operator of the mesh computed according to [15], $LAPL_i, i = \{1, \ldots, 6\}$, (Figure 2(f-i));
- a mix of the first three eigenfunctions of the Laplace-Beltrami operator obtained according to the rule: $MIX_{i+j-2} = (LAPL_i)^2 - (LAPL_j)^2$, $i = \{1, 2\}$, $j = \{2, 3\}$, $i \neq j$ (Figure 2(j-l)).

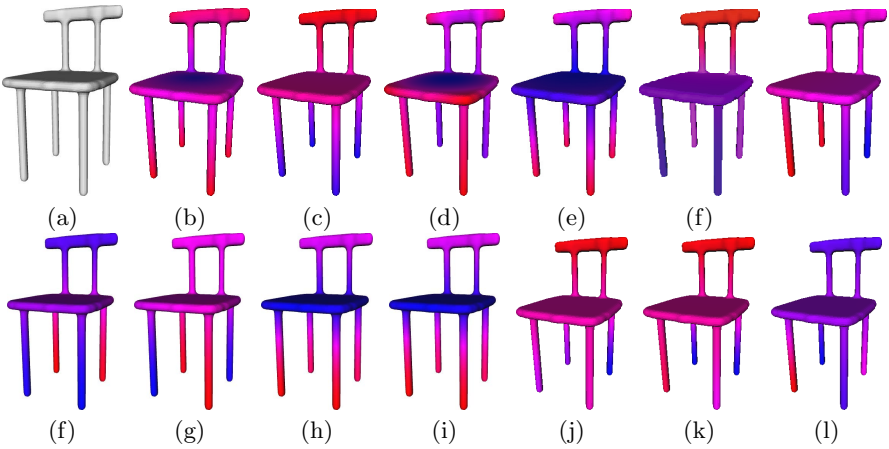

Fig. 2. The set of real functions in our framework. Colors represent the function, from low (blue) to high (red) values.

Each function reflects either intrinsic or extrinsic shape features. Geodesic-based and Laplacian-based functions are isometry-invariant and therefore pose invariant because they approximate the intrinsic Riemannian metric of the surface [16]. In this way, the graph representation is independent of the different articulations of the objects. On the other hand, the distance from the barycentre highlights the distribution of the object with respect to its barycentre. Therefore such a function is rotation invariant with respect to rotations around the barycentre but sensitive to pose variations. Similarly the distances from the principal shape axis and its orthogonal are independent of axis rotations and independent of axis symmetries.

Mixing the different properties (rigid or isometry invariant) different shape features are kept.

3 Heat Flow Complexity in Digraphs

3.1 The Laplacian of a Directed Graph

A directed graph (digraph) $G = (V, E)$ with $n = |V|$ vertices and edges $E \subseteq V \times V$ is encoded by and adjacency matrix $\mathbf{A}$ where $A_{ij} > 0$ if $i \to j \in E$ and $A_{ij} = 0$ otherwise (this definition includes weigthed adjacency matrices). The outdegree matrix $\mathbf{D}$ is a diagonal matrix where $D_{ii} = \sum_{j \in V} A_{ij}$. The transition matrix $\mathbf{P}$ is defined by $P_{ij} = \frac{A_{ij}}{D_{ii}}$ if $(i, j) \in E$ and $P_{ij} = 0$ otherwise. The transition matrix is key to defining random walks on the digraph and P_{ij} is the probability of reaching node j from node i. Given these definitions we have that $\sum_{j \in V} P_{ij} \neq 1$ in general. In addition, $\mathbf{P}$ is irreducible iff G is strongly connected (there is path from each vertex to every other vertex). If $\mathbf{P}$ is irreducible, the Perron-Frobenius theorem ensures that there exists a left eigenvector ϕ satisfying $\phi^T \mathbf{P} = \lambda \phi^T$ and $\phi(i) > 0 \, \forall i$. If $\mathbf{P}$ is aperiodic (spectral radius $\rho = 1$) we have $\phi^T \mathbf{P} = \rho \phi^T$ and all the other eigenvalues have an absolute value smaller that $\rho = 1$. By ensuring strong connection and aperiodicity we also ensure that any random walk in a directed graph satisfying these two properties converges to a unique stationary distribution.

Normalizing ϕ so that $\sum_{i \in V} \phi(i) = 1$, we encode the eigenvector elements as a probability distribution. This normalized row vector ϕ corresponds to the stationary distribution of the random walks defined by $\mathbf{P}$ since $\phi \mathbf{P} = \phi$. Therefore, $\phi(i) = \sum_{j, j \to i} \phi(j) P_{ji}$, that is, the probability of that the random walk is at node i is the sum of all incoming probabilities from all nodes j satisfying $j \to j$. If we define $\Phi = diag(\phi(1) \dots \phi(n))$ we have the definition of the following matrices:

$$\mathbf{L} = \Phi - \frac{\Phi \mathbf{P} + \mathbf{P}^T \Phi}{2} \quad \text{and} \quad \mathcal{L} = I - \frac{\Phi^{1/2} \mathbf{P} \Phi^{-1/2} + \Phi^{-1/2} \mathbf{P}^T \Phi^{1/2}}{2}, \qquad (1)$$

where $\Phi = diag(\phi(1) \dots \phi(n))$, $\mathbf{L}$ is the *combinatorial directed Laplacian* and $\mathcal{L}$ is the *normalized directed Laplacian* [17].

Symmetrizing $\mathbf{P}$ leads to real valued eigenvalues and eigenvectors. In any case, satisfying irreducibility is difficult in practice since sink vertices may arise frequently. A formal trick for solving this problem consists of replacing $\mathbf{P}$ by $\mathbf{P}'$ so that $P'_{ij} = \frac{1}{n}$ if $A_{ij} = 0$ and $D_{ii} = 0$. This strategy is adopted in Pagerank [18] and allows for *teleporting* acting on the random walk to any other node in the graph. Teleporting is modeled by redefining $\mathbf{P}$ in the following way: $\mathbf{P} = \eta\mathbf{P}' + (1-\eta)\frac{\mathbf{1}\mathbf{1}^T}{n}$ with $0 < \eta < 1$. The new $\mathbf{P}$ ensures both irreducibility and aperiodicity and this allows us to both apply $\mathbf{P}'$ with probability η and to teleport from any node with $A_{ij} = 0$ with probability $1 - \eta$. In [19] a trade-off between large values η (preserving more the structure of $\mathbf{P}'$) and small ones (potentially increasing the spectral gap) is recommended. For instance, in [20], where the task is to learn classifiers on directed graphs, the setting is $\eta = 0.99$. When using the new $\mathbf{P}$ we always have that $P_{ii} \neq 0$ due to the Pagerank masking. Such masking may introduce significant interferences in heat diffusion when the Laplacian is used to derive the heat kernel.

3.2 Directed Heat Kernels and Heat Flow

We commence by reviewing the concept of *heat flow* [6]. Firstly, the spectral decomposition of the diffusion kernel is $\mathbf{K}_\beta(G) = \exp(-\beta\mathcal{L}) \equiv \Psi\Lambda\Psi^T$, where $\Lambda = diag(e^{-\beta\lambda_1}, e^{-\beta\lambda_2}, \ldots, e^{-\beta\lambda_n})$, $\Psi = [\psi_1, \psi_2, \ldots, \psi_n]$, and $\{(\lambda_i, \psi_i)\}_{i=1}^n$ are the eigenvalue-eigenvector pairs of $\Phi - \mathbf{W}$ where $\mathbf{W} = \frac{\Phi\mathbf{P} + \mathbf{P}^T\Phi}{2}$ can be seen as the *weight matrix* of the undirected graph G_u associated with G. Anyway, $K_{\beta_{ij}} = \sum_{k=1}^n \psi_k(i)\psi_k(j)e^{-\lambda_k\beta}$, and $K_{\beta_{ij}} \in [0,1]$ is the (i,j) entry of a doubly stochastic matrix. Doubly stochasticity for all β implies *heat conservation* in the system as a whole. That is, not only in the nodes and edges of the graph but also in the *transitivity links* eventually established between non-adjacent nodes (if i is not adjacent to j, eventually will appear an entry $K_{\beta_{ij}} > 0$ for β large enough). The total *directed heat* flowing through the graph at a given β *(instantaneous directed flow)* is given by

$$\mathcal{F}_\beta(G) = \sum_{i \to j} A_{ij} \left(\sum_{k=1}^n \psi_k(i)\psi_k(j)e^{-\lambda_k\beta} \right) , \tag{2}$$

A more compact definition of the flow is $\mathcal{F}_\beta(G) = \mathbf{A} : \mathbf{K}_\beta$, where $\mathbf{X} : \mathbf{Z} = \sum_{ij} X_{ij}Z_{ij} = trace(\mathbf{X}\mathbf{Z}^T)$ is the Frobenius inner product. While instantaneous flow for the heat flowing through the edges of the graph, it accounts neither for the heat remaining in the nodes nor for that in the transitivity links. The limiting cases are $\mathcal{F}_0 = 0$ and $\mathcal{F}_{\beta_{max}} = \frac{1}{n}\sum_{i \to j} A_{ij}$ which is reduced to $\frac{|E|}{n}$ if G is unattributed ($A_{ij} \in \{0,1\}\ \forall ij$). Defining $\mathcal{F}_\beta$ in terms of $\mathbf{A}$ instead of $\mathbf{W}$, we retain the *directed* nature of the original graph G. The function derived from computing $\mathcal{F}_\beta(G)$ from $\beta = 0$ to β_{max} is the so called *directed heat flow trace*. These traces satisfy the *phase transition principle* [6] (although the formal proof is out of the scope of this paper). In general heat flow diffuses more slowly than in the undirected case and phase transition points (PTPs) appear later. This is due to the constraints imposed by $\mathbf{A}$.

3.3 Thermodynamic Depth Complexity

Let $G = (V, E)$ with $|V| = n$. Then the *directed history of a node* $i \in V$ is $h_i(G) = \{e(i), e^2(i)), \ldots, e^p(i)\}$ where: $e(i) \subseteq G$ is the *first-order expansion subgraph* given by i and all $j : i \to j$. If there are nodes j also satisfying $j \to i$ then these edges are included. If node i is a sink then $e(i) = i$. Similarly $e^2(i) = e(e(i)) \subseteq G$ is the *second-order expansion* consisting on $j \to z : j \in V_{e(i)}, z \notin V_{e(i)}$, including also $z \to j$ if these edges exists and $j \to z$. This process continues until p cannot be increased. If G is strongly connected $e^p(i) = G$, otherwise $e^p(i)$ is the strongly connected component to which i belongs. Thus, every $h_i(G)$ defines a different causal trajectory which may lead to G itself if it is strongly connected. The *depth* of such macro-states relies on the variability of the causal trajectories leading to them. In order to characterize each trajectory we combine the heat flow complexities of its expansion subgraphs by means of defining *minimal enclosing Bregman balls* (MEBB) [21]. Here we use the I-Kullback-Leibler (I-KL) Bregman divergence between traces f and g: $D_F(\boldsymbol{f}||\boldsymbol{g}) = \sum_{i=1}^{d} f_i \log \frac{f_i}{g_i} - \sum_{i=1}^{d} f_i + \sum_{i=1}^{d} g_i$ with convex generator $F(\boldsymbol{f}) = \sum_{i=1}^{d}(f_i \log f_i - f_i)$.

Given $h_i(G)$, the heat flow complexity trace $\boldsymbol{f}_t = \mathcal{F}(e^t(i))$ for the $t-th$ expansion of i, a generator F and a Bregman divergence D_F, the *causal trajectory* leading to G (or one of its strongly connected components) from i is characterized by the center $\boldsymbol{c}_i \in R^d$ and radius $r_i \in R$ of the MEBB $\mathcal{B}^{\boldsymbol{c}_i, r_i} = \{\boldsymbol{f}_t \in \mathcal{X}_i : D_F(\boldsymbol{c}_i||\boldsymbol{f}_t) \leq r_i\}$ where $\mathcal{X}$ is the set of all causal trajectories for the $i-$th node.Solving for the center and radius implies finding $\boldsymbol{c}^*$ and r^* minimizing r subject to $D_F(\boldsymbol{c}_i||\boldsymbol{f}_t) \leq r \ \forall t \in \mathcal{X}_i$ with $|\mathcal{X} : i| = T$. Considering the Lagrange multipliers α_t we have that $\boldsymbol{c}^* = \nabla^{-1} F(\sum_{t=1}^{T} \alpha_t \boldsymbol{f}_t \nabla F(\boldsymbol{f}_t))$. The efficient algorithm in [21] estimates both the center and multipliers. This idea is closely related to Core Vector Machines [22], and it is interesting to focus on the non-zero multipliers (and their support vectors) used to compute the optimal radius. More precisely, the multipliers define a convex combination and we have $\alpha_t \propto D_F(\boldsymbol{c}^*||\boldsymbol{f}_t)$, and the radius is simply chosen as: $r^* = \max_{\alpha_t > 0} D_F(\boldsymbol{c}^*||\boldsymbol{f}_t)$. Given the directed graph $G = (V, E)$, with $|V| = n$ and all the n pairs $(\boldsymbol{c}_i, r_i)$, the *heat flow-thermodynamic depth complexity* of G is characterized by the MEBB $\mathcal{B}^{\boldsymbol{c}, r} = \{\boldsymbol{c}_i \in \mathcal{X}_i : D_F(\boldsymbol{c}||\boldsymbol{c}_i) \leq r\}$. As a result, the *TD depth of the directed graph* is given by $\mathcal{D}(G) = r$.

4 Experiments

In order to compare our method with the technique proposed in [8] we use the same database, SHRECH version used in the Shape Retrieval Contest in [23]. The database has 400 exemplars and 20 classes (20 exemplars per class). For each exemplar we apply the 13 real functions presented in Section 2 and then extract the corresponding Reeb digraphs. Then, each exemplar is characterized by 13 the heat flow complexities (one per digraph). If we map these vectors (bags of complexities) via MDS we found that it is quite easy to discriminate glasses from pliers and fishes. However, it is very difficult to discriminate humans from chairs

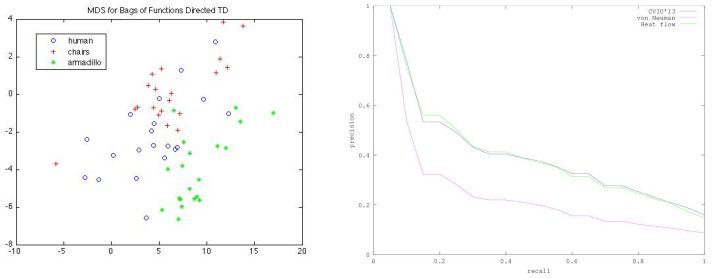

Fig. 3. Experiments. Left: MDS for humans, chairs and armadillos. Right: PR curves.

(see Figure 3-left). The average behavior of these bags of complexities is given by the precision recall (PR) curves. In Figure 3-right we show the PR curves for Feature Selection [8] (CVIU'13), Thermodynamic Depth (TD) with the von Neumann Entropy (here we use the **W** attributed graph induced by the Directed Laplacian) and TD with directed heat flow. Our PR (heat flow) as well as the one of Feature Selection reaches the average performance of attributed methods. The 10-fold CV error for 15 classes reported by Feature Selection is $23,3\%$. However, here we obtain a similar PR curve for the 20 class problem. Given that Feature Selection relies on a complex offline process, the less computationally demanding heat flow TD complexity for digraphs produces comparable results (or better ones, if we consider that we are addressing the 20 class problem). In addition, heat flow outperforms von Neumann entropy when embedded in TD.

5 Conclusions and Future Work

The main contribution of this paper is the proposal of a method (fusion of digraphs heat flow complexity) which has a similar discrimination power (or even better if we consider the whole 20 classes problem) than Feature Selection and outperforms von Neumann entropy. Future works include the exploration of more sophisticated methods for fusing complexities and more real functions.

Acknowledgements. Francisco Escolano was funded by project TIN2012-32839 of the Spanish Government. Edwin Hancock was supported by a Royal Society Wolfson Research Merit Award.

References

[1] Torsello, A., Hancock, E.R.: Learning Shape-Classes Using a Mixture of Tree-Unions. IEEE Tran. on Pattern Analysis and Mach. Intelligence 28(6), 954–967 (2006)

[2] Torsello, A., Lowe, D.L.: Supervised Learning of a Generative Model for Edge-Weighted Graphs. In: Proc. of ICPR (2008)

[3] Passerini, F., Severini, S.: The von Neumann Entropy of Networks. arXiv:0812.2597v1 (December 2008)
[4] Han, L., Escolano, F., Hancock, E.R., Wilson, R.: Graph Characterizations From Von Neumann Entropy. Pattern Recognition Letters (2012) (in press)
[5] Lloyd, S., Pagels, H.: Complexity as Thermodynamic Depth Ann. Phys. 188, 186 (1988)
[6] Escolano, F., Hancock, E.R., Lozano, M.A.: Heat Diffusion: Thermodynamic Depth Complexity of Networks. Phys. Rev. E 85, 036206 (2012)
[7] Escolano, F., Bonev, B., Hancock, E.R.: Heat Flow-Thermodynamic Depth Complexity in Directed Networks. In: Gimel'farb, G., Hancock, E., Imiya, A., Kuijper, A., Kudo, M., Omachi, S., Windeatt, T., Yamada, K. (eds.) SSPR & SPR 2012. LNCS, vol. 7626, pp. 190–198. Springer, Heidelberg (2012)
[8] Bonev, B., Escolano, F., Giorgi, D., Biasotti, S.: Information-theoretic Selection of High-dimensional Spectral Features for Structural Recognition. Computer Vision and Image Understanding 117(3), 214–228 (2013)
[9] Reeb, G.: Sur les points singuliers d'une forme de Pfaff complètement intégrable ou d'une fonction numérique. Comptes Rendus Hebdomadaires des Séances de l'Académie des Sciences 222, 847–849 (1946)
[10] Biasotti, S., Giorgi, D., Spagnuolo, M., Falcidieno, B.: Reeb graphs for shape analysis and applications. Theoretical Computer Science 392(1-3), 5–22 (2008)
[11] Biasotti, S.: Topological coding of surfaces with boundary using Reeb graphs. Computer Graphics and Geometry 7(3), 31–45 (2005)
[12] Biasotti, S.: Computational Topology Methods for Shape Modelling Applications. PhD Thesis, Universitá degli Studi di Genova (May 2004)
[13] Biasotti, S., De Floriani, L., Falcidieno, B., Frosini, P., Giorgi, D., Landi, C., Papaleo, L., Spagnuolo, M.: Describing shapes by geometrical-topological properties of real functions. ACM Comput. Surv. 40(4), 1–87 (2008)
[14] Hilaga, M., Shinagawa, Y., Kohmura, T., Kunii, T.L.: Topology Matching for Fully Automatic Similarity Estimation of 3D Shapes. In: Proc. of SIGGRAPH 2001, pp. 203–212 (2001)
[15] Belkin, M., Sun, J., Wang, Y.: Discrete Laplace Operator for Meshed Surfaces. In: Proc. Symposium on Computational Geometry, pp. 278–287 (2008)
[16] Bronstein, A.M., Bronstein, M.M., Kimmel, R.: Efficient Computation of Isometry-Invariant Distances Between Surfaces. SIAM J. Sci. Comput. 28(5), 1812–1836 (2006)
[17] Chung, F.: Laplacians and the Cheeger Inequailty for Directed Graphs. Annals of Combinatorics 9, 1–19 (2005)
[18] Page, L., Brin, S., Motwani, R., Winograd, T.: The PageRank Citation Ranking: Bring Order to the Web (Technical Report). Stanford University (1998)
[19] Johns, J., Mahadevan, S.: Constructing Basic Functions from Directed Graphs for Value Functions Approximation. In: Proc. of ICML (2007)
[20] Zhou, D., Huang, J., Schölkopf, B.: Learning from Labeled and Unlabeled Data on a Directed Graph. In: Proc. of ICML (2005)
[21] Nock, R., Nielsen, F.: Fitting the Smallest Enclosing Bregman Ball. In: Gama, J., Camacho, R., Brazdil, P.B., Jorge, A.M., Torgo, L. (eds.) ECML 2005. LNCS (LNAI), vol. 3720, pp. 649–656. Springer, Heidelberg (2005)
[22] Tsang, I.W., Kocsor, A., Kwok, J.T.: Simple Core Vector Machines with Enclosing Balls. In: Proc. of ICLM (2007)
[23] Giorgi, D., Biasotti, S., Paraboschi, L.: SHape Retrieval Contest: Watertight Models Track, `http://watertight.ge.imati.cnr.it`